SL1 region and extending to the very 5′ end of HCV RNA (Fig. 1A). This region has been shown to be essential for HCV RNA replication (14, 19). Two proteins, Ago2 and PCBP2, are known to associate with this region: Ago2 is recruited by miR-122, whereas PCBP2 has been suggested to bind to SL1, a small stem-loop near the 5′ end (9, 14, 20). In the present study, we sought to identify additional proteins associating with this region of the HCV genome, either dependently or independently of miR-122, and to assess their function in HCV replication. We found that hnRNP L and IGF2BP1 bind to single-stranded RNA (ssRNA) representing the extreme 5′ end of the HCV genome, whereas DHX9, ADAR1, and NF90 associate with the cognate double-stranded RNA (dsRNA). Among these proteins, hnRNP L and NF90 are shown to be required for efficient HCV replication but not HCV IRES-directed translation. Both proteins bind viral RNA in infected cells and may be associated with viral replication complexes.

MATERIALS AND METHODS

Cells, reagents, and plasmids. Huh-7.5 cells (obtained from Charles Rice, Rockefeller University) and FT3-7 cells were maintained as described previously (8, 21). U2OS cells with conditional expression of the HCV NS5A protein were kindly provided by Darius Moradpour (Université de Lausanne) (22). WST-1 reagent (Millipore) was used to monitor cell proliferation according to the manufacturer's suggested protocol. Plasmids pH77S.3/GLuc2A and pHJ3-5 (both infectious HCV molecular clones) have been described previously (8, 23). pHCVΔC-GLuc expresses an HCV "minigenome" comprised of RNA sequence encoding the first 12 amino acids of the HCV core protein fused at its downstream end to the *Gaussia princeps* luciferase (GLuc) sequence and flanked by the 5′ and 3′ untranslated RNA sequences of H77S, a genotype 1a virus (24).

RNA transcription. Viral RNAs were transcribed *in vitro* as described previously (9).

Biotinylated RNA pull-down. Oligoribonucleotide baits, H77S 1-47 and S1/S2p6 (Fig. 1A), representing the 5′ 47 nucleotides of wild-type genotype 1 HCV RNA and a related S1/S2p6 mutant (see below) and conjugated to biotin at their 3′ ends, were synthesized by Dharmacon (Pittsburgh, PA). These RNA baits (10 pmol in each reaction) were incubated alone or with 10 pmol of a similarly synthesized complementary antisense oligonucleotide (to generate a dsRNA bait) or variable amounts of single-strand synthetic miR-122 (9), heated at 75°C for 5 min, and then cooled to room temperature. Annealed RNAs were bound to magnetic streptavidin T1 beads (Invitrogen) according to the manufacturer's instructions and then incubated with Huh-7.5 cell cytoplasmic lysate for 1 h at 4°C. Anti-miR-122 or anti-random locked nucleic acid (LNA) oligonucleotides (9) were added to the lysate where indicated. Proteins bound to the beads were eluted with SDS-PAGE sample buffer, resolved by SDS-PAGE and subjected to SYPRO Ruby staining or immunoblotting with specific antibodies. Specific bands were cut from the gel and proteins in each identified by mass spectrometry with the UNC Proteomics Core Facility.

Transfections. siRNA pools targeting IGF2BP1, hnRNP L, ADAR1, DHX9, NF90, and control small interfering RNA (siRNA) pools (Dharmacon) were transfected using siLentfect lipid reagent (Bio-Rad). *In vitro*-transcribed HCV RNA (1.25 μg) was transfected into 2.5×10^6 Huh-7.5 cells using the TransIT mRNA kit (Mirus Bio).

Real-time reverse transcription-PCR (RT-PCR). To quantify HCV RNA, cDNA was produced by reverse transcription of RNA using oligo(dT) and an HCV-specific primer (5′-GGCCAGTATCAGCACTCTC TGCAGTC-3′) targeting the 3′UTR of the genome and SuperScript III reverse transcriptase (Invitrogen). Quantitative PCR analysis was carried out using iTaq SYBR green Supermix with the CFX96 system (Bio-Rad). HCV RNA abundance was determined by reference to a standard curve using PCR primers targeting the 5′UTR (5′-CATGGCGTTAGTATGAG TGTCGT-3′ and 5′-CCCTATCAGGCAGTACCACAA-3′) and normalized to the abundance of β-actin mRNA (primers 5′-GTCACCGGAGTC CATCACG-3′ and 5′-GACCCAGATCATGTTTGAGACC-3′). The HCV minigenome RNA was amplified by the primers 5′-CACGCCCAAGATG AAGAAGT-3′ and 5′-GAACCCAGGAATCTCAGGAATG-3′.

Immunoblots. Immunoblotting was carried out according to standard methods with the following antibodies: mouse monoclonal antibody (MAb) to β-actin (AC-74; Sigma-Aldrich); rat MAb to Ago2 (Sigma-Aldrich); rabbit polyclonal antibodies to ADAR1, NF90, and DHX9 (Bethyl Laboratory); mouse MAb to hnRNP L (Millipore); rabbit polyclonal antibody to IGF2BP1 (Abcam); mouse MAb to PCBP2 (Abnova); mouse MAb to hnRNP C and PTB (Abcam); MAb to HCV core protein (Pierce); and rabbit polyclonal antibody to HCV NS5A protein (kindly provided by Takaji Wakita). Protein bands were visualized with an Odyssey infrared imaging system (Li-Cor Biosciences).

***Gaussia* luciferase (GLuc) assay.** Cell culture supernatant fluids were collected at intervals after RNA transfection, and cells were refed with fresh media. Secreted GLuc activity was measured in the supernatant fluids using the Biolux *Gaussia* luciferase assay kit (New England BioLabs) as previously described (23).

Infectious virus titration. Supernatant fluids (100 μl) from HJ3-5 virus-infected cells were incubated with 5×10^4 uninfected Huh-7.5 cells in a 48-well plate for 6 h. After replacement of media, cells were allowed to grow for 72 h before fixation and immunolabeling with anti-core antibody (Pierce). Foci of infected cells were visualized and infectious virus titer quantified in terms of focus-forming units as described previously (24).

Preparation of cytoplasmic and nuclear lysates. Huh-7.5 cells were harvested in lysis buffer A (150 mM KCl, 25 mM Tris-HCl [pH 7.5], 5 mM EDTA,1% Triton X-100, 2 mM dithiothreitol, Complete protease inhibitor mixture [Roche, Mannheim, Germany]). Lysates were centrifuged for 5 min at 1,000 × *g* at 4°C. The supernatants were collected as a cytoplasmic lysate. The nuclear pellet was washed with phosphate-buffered saline and lysed in buffer B (500 mM KCl, 25 mM Tris-HCl [pH 7.5], 2 mM EDTA, 1% NP-40, 0.1% SDS, Complete protease inhibitor mixture). Cytoplasmic and nuclear lysates were cleared by centrifugation at 17,000 × *g* for 10 min at 4°C.

Immunoprecipitation. Cytoplasmic lysates of HJ3-5 virus-infected Huh-7.5 cells were incubated with anti-hnRNP L (Millipore), anti-NF90 (Bethyl Labs), anti-Dcp1a (Abnova), rabbit anti-NS5A (kindly provided by T. Wakita), or isotype control IgG at 4°C for 2 h, followed by addition of 30 μl of protein G-Sepharose (GE Healthcare) for 1 h. RNase A was added to the lysate where indicated. The Sepharose beads were washed three times in lysis buffer. Proteins were eluted with SDS-PAGE sample buffer and subjected to SDS-PAGE, followed by immunoblotting. Coprecipitated RNAs were extracted using the RNeasy minikit (Qiagen). HCV RNA was detected by reverse transcription-PCR (RT-PCR) using the SuperScript One-Step RT-PCR (Invitrogen) and the specific primers 5′-CA TGGCGTTAGTATGAGTGTCGT-3′ and 5′-CCCTATCAGGCAGTAC CACAA-3′.

Membrane flotation assay. The membrane flotation assay was carried out according the method of Okamoto et al. (25) with some modifications. Eight million FT3-7 cells with or without HJ3-5 virus infection were harvested, suspended in 1 ml of TNE buffer (25 mM Tris-HCl [pH 7.4] containing 150 mM NaCl, 5 mM EDTA, and Complete protease inhibitor cocktail), and then disrupted by 20 passages through a 25-gauge needle. After low-speed centrifugation (1,000 × *g*), postnuclear supernatants were divided into two tubes and incubated for 30 min on ice with or without 0.5% Triton X-100. The lysates were mixed with 1.2 ml of an iodixanol (OptiPREP; Sigma-Aldrich, St. Louis, MO) solution with a final concentration of 45%. This mixture was overlaid with a 35 to 10% iodixanol gradient and then centrifuged at 42,000 rpm and 4°C for 14 h in an SW55 Ti rotor (Beckman Coulter, Fullerton, CA). Twelve fractions were collected from the top of the gradient and precipitated with trichloroacetic acid, followed by acetone washing. Dried pellets were resolved in the loading buffer, boiled, and subjected to SDS-PAGE, followed by immu-

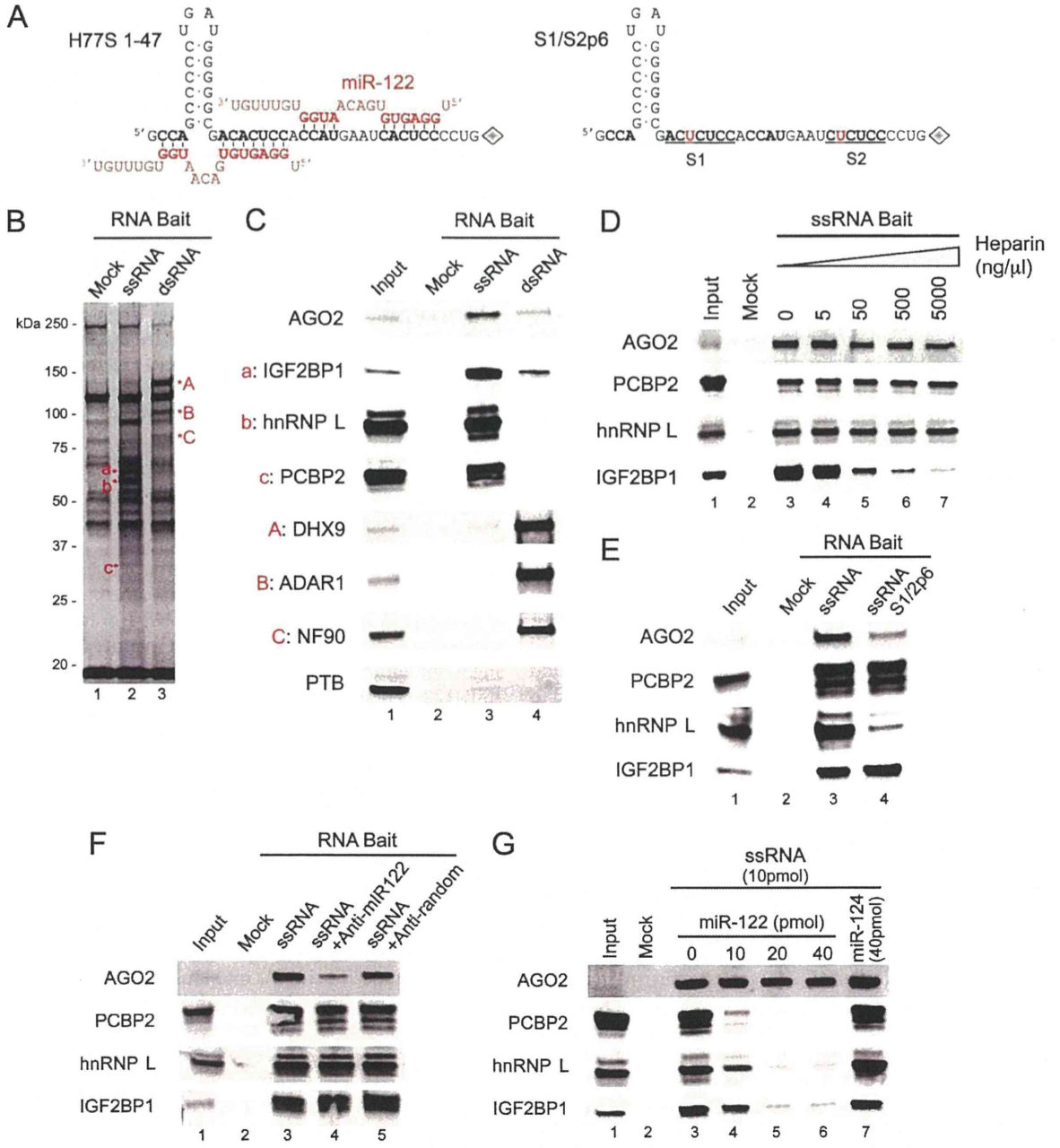

FIG 1 Identification of proteins binding to the 5′ end of the HCV 5′UTR. (A) RNA baits used in the pulldown experiments. (Left) ssRNA oligonucleotide representing the 5′ most 47 bases in the HCV genome (H77S virus, black font). Two copies of miR-122 (red font) are shown bound to the probe as determined by prior genetic studies (21). Positions involved in base-pairing are shown in boldface. (Right) S1/S2p6, a related bait with base substitutions (red font) at position 6 of the two miR-122 seed sequence binding sites, S1 and S2 (underlined). RNA probes were conjugated to biotin (diamond symbol) at their 3′ ends. (B) RNA pulldown. Synthetic biotinylated RNA bait (H77S 1-47) was incubated with Huh-7.5 cytoplasmic lysate by itself (ssRNA bait) or after being preannealed with a complementary negative-strand RNA (dsRNA bait). Proteins pulled down were resolved by SDS-PAGE and stained by SYPRO Ruby. Unique protein bands in each lane indicated by asterisks were identified by mass spectrometry. Mock, no RNA bait. (C) Protein samples from panel B were subjected to immunoblot analysis with specific antibodies. 2% input lysate was loaded as reference. Ago2, IGF2BP1, hnRNP L and PCBP2 bind preferentially to ssRNA bait, while DHX9, ADAR1, and NF90 bind to dsRNA bait. PTB was detected as a negative control. (D) RNA pulldown assay was done as in panel B using ssRNA bait in the presence of the indicated amount of heparin. Ago2, PCBP2, IGF2BP1, and hnRNP L proteins were detected by immunoblotting. Heparin inhibited the binding of IGF2BP1, but not the other proteins. (E) RNA pulldown assay was performed as in panel B using RNA bait containing single mutations in S1 and S2 site (S1/2p6, see panel A). S1/S2p6 RNA demonstrated reduced binding of Ago2 and hnRNP L but not IGF2BP1 and PCBP2. (F) RNA pulldown assay was carried out as in panel B except that anti-miR-122 or anti-random oligonucleotides were added to the lysate. Ago2, PCBP2, IGF2BP1, and hnRNP L proteins were detected by immunoblotting. Anti-miR-122 blocked the binding of Ago2 but not the other proteins. (G) RNA pulldown assay was carried out as in panel B except that 10 pmol of ssRNA bait was preannealed with the indicated amount of single-strand miR-122 or miR-124. Ago2, PCBP2, IGF2BP1, and hnRNP L proteins were detected by immunoblotting. The addition of miR-122 blocked the binding of PCBP2, IGF2BP1, and hnRNP L but not Ago2.

noblotting. Protease treatment was carried out with 1 μg of proteinase K per 50-μl fraction sample with or without 1% NP-40 and then incubated at 37°C for 30 min.

Statistical tests. Statistical significance was calculated using Prism 5 for Mac OS X (GraphPad Software, Inc.) and specific statistical tests as indicated.

RESULTS

To identify proteins that bind to the 5′ terminus of positive-strand HCV RNA, we used a biotin-tagged RNA pulldown strategy. A synthetic oligonucleotide representing the 5′ 47 nucleotides of genotype 1 H77 virus was conjugated to biotin at its 3′ end (Fig. 1A, left). This RNA bait (ssRNA bait) was incubated with Huh-7.5 cell cytoplasmic lysate. Since double-strand RNA is an important intermediate in HCV RNA replication, we also sought to isolate proteins that bind to a double-stranded version of this bait by preannealing it with a complementary negative-strand RNA oligonucleotide (dsRNA bait). The proteins associated with these baits were pulled down with streptavidin beads, resolved by SDS-PAGE, and visualized by SYPRO Ruby staining (Fig. 1B). Specific bands that were pulled down by ssRNA or dsRNA bait were cut from the gel and identified by mass spectrometry. We identified three proteins that specifically associated with the ssRNA bait (Fig. 1B, lane 2, bands a, b, and c). These were identified by mass spectrometry as insulin-like growth factor 2 mRNA binding protein 1 (IGF2BP1), heterogeneous nuclear ribonucleoprotein L (hnRNP L), and PCBP2, respectively. Three bands that specifically bound the dsRNA bait (Fig. 1B, lane 3, bands A, B, and C) were found to be DEAH box helicase 9 (DHX9, also known as ATP-dependent RNA helicase 9), dsRNA-specific adenosine deaminase (ADAR1), and "nuclear factor of activated T cells 90 kDa" (NF90; also known as interleukin enhancer-binding factor 3 [ILF3]). To confirm the mass spectrometry results, we used immunoblotting with specific antibodies to these proteins. Consistently, we detected specific binding of IGF2BP1, hnRNP L, and PCBP2 to the ssRNA bait and binding of DHX9, ADAR1, and NF90 to the dsRNA bait (Fig. 1C).

As the 5′ HCV RNA sequence contains both miR-122 binding sites, we anticipated that endogenous miR-122 would bind with Ago2 protein to the ssRNA bait (9). This was confirmed in immunoblots (Fig. 1C), although Ago2 was not visible by SYPRO Ruby staining due to low abundance or inefficient binding of endogenous miR-122 to the bait. In contrast, PTB, an RNA-binding protein required for HCV replication (16), did not appear to bind either ssRNA or dsRNA bait in our assay and served as a negative control (Fig. 1C). IGF2BP1, hnRNP L, and PCBP2 are all RNA-binding proteins. PCBP2 has been shown to bind to the SLI region of the HCV 5′UTR and to be required for HCV replication (14, 20). IGF2BP1 has also been found to bind to the 5′ sequence of HCV RNA and to modulate HCV IRES function (26, 27). hnRNP L is a novel factor identified in our assay that has not been shown previously to bind the 5′ end of HCV RNA. DHX9, ADAR1, and NF90 all contain double-strand RNA-binding motifs, which is consistent with their binding to the dsRNA bait. DHX9 has RNA helicase activity, ADAR1 is an RNA specific adenosine deaminase, and NF90 was first discovered as a subunit of a nuclear transcription factor complex (28). Their function in HCV replication has not been well studied. To test the specificity of the interaction between these RNA-binding proteins and the bait, we repeated the ssRNA pulldown assay in the presence of a nonspecific competitor, heparin (Fig. 1D). Increasing amounts of heparin reduced the binding of IGF2BP1 but had little effect on the binding of Ago2, PCBP2, or hnRNP L, confirming that Ago2 (miR-122), PCBP2 and hnRNP L interact with the HCV 5′ terminal sequence in a specific and likely sequence-dependent manner.

To determine whether the binding of IGF2BP1, hnRNP L, and PCBP2 to the HCV 5′ sequence is dependent on binding of miR-122, such as Ago2 (9), we repeated the pulldown assay using a mutant RNA bait that contains a single base substitution in both the S1 and the S2 sites (Fig. 1A, right, S1/2p6) that significantly reduces miR-122 binding. As expected (9), the mutation substantially reduced Ago2 binding (Fig. 1E). Interestingly, it also diminished binding of hnRNP L but not PCBP2 or IGF2BP1 (Fig. 1E), which suggests that hnRNP L binding might be dependent on miR-122. To assess this further, we carried out a pulldown assay in the presence of an antisense anti-miR-122 locked nucleic acid (LNA) oligonucleotide. However, while the antagomir dramatically reduced Ago2 binding to the ssRNA bait, there was no effect on the binding of any of the other proteins, indicating that they bind to HCV RNA independently of miR-122 (Fig. 1F). Therefore, the reduced binding of hnRNP L to the p6 mutant RNA is unlikely to be due to reduced miR-122 binding and is more likely caused by direct disruption of the hnRNP L binding site. If this is the case, it indicates that hnRNP L binds to the same or overlapping site as the miR-122 seed sequence. Indeed, when we preannealed miR-122 to the ssRNA bait, the binding of hnRNP L was dramatically decreased in a miR-122 dose-dependent manner (Fig. 1G). Surprisingly, the binding of IGF2BP1 and PCBP2 was also blocked by miR-122. These data indicate that IGF2BP1, hnRNP L, and PCBP2 bind the HCV 5′ sequence in competition, not in cooperation with miR-122. This is not surprising given the extensive interactions of miR-122 with this segment of the viral genome (Fig. 1A, left).

We next sought to determine whether proteins that bind the 5′ end of HCV RNA have a function in HCV replication. Since Ago2 and PCBP2 have already been demonstrated to be required for HCV replication, we focused on the other proteins detected in our pulldown assay, including IGF2BP1, hnRNP L, ADAR1, DHX9, and NF90. We knocked down the expression of these proteins by transfecting specific siRNAs into Huh-7.5 cells (Fig. 2A) and then transfected a modified HCV genomic RNA that expresses *Gaussia princeps* luciferase (GLuc) as a reporter. Secreted GLuc activity was monitored over 72 h as an indicator of HCV replication (9). siRNA-mediated depletion of hnRNP L and NF90 substantially reduced HCV replication. Depletion of IGF2BP1 and DHX9 caused much smaller but nonetheless reproducible and statistically significant reductions in replication, while ADAR depletion was without effect (Fig. 2B). These results suggested that, among these RNA-binding proteins, hnRNP L and NF90 may be particularly important for efficient HCV replication. However, depletion of either protein also caused significant defects in cell proliferation as measured by WST-1 assay, in both cases reducing cell growth by ca. 25% (Fig. 2C).

Further studies focused on hnRNP L and NF90. To minimize the impact of their depletion on cell growth, we repeated the RNA interference experiments in cells cultured in media containing 2% serum (Fig. 3). HCV replication was significantly reduced by depletion of either protein, as measured by GLuc activity (Fig. 3A). Total HCV RNA abundance was also reduced by ca. 60%, after hnRNP L depletion and 40% after NF90 depletion (Fig. 3B). Importantly, hnRNP L and NF90 depletion resulted in little change

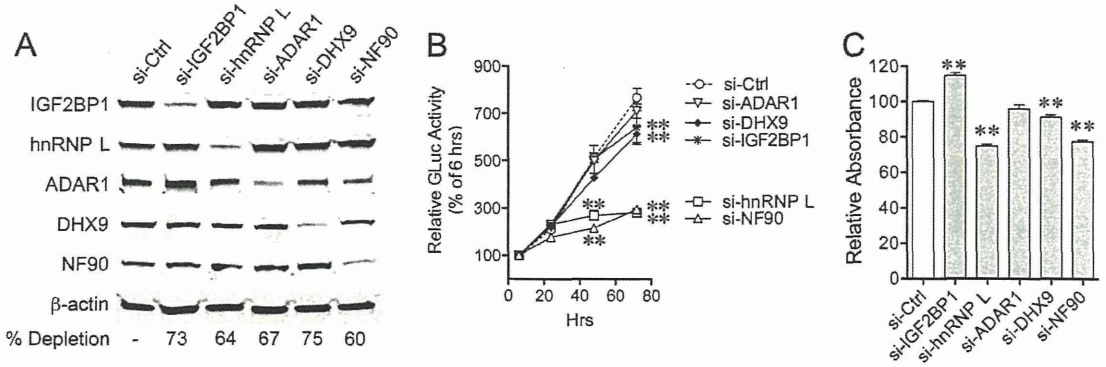

FIG 2 Depletion of hnRNP L or NF90 impairs HCV replication. Huh-7.5 cells were transfected with siRNAs targeting the indicated proteins or scrambled si-Ctrl and then 48 h later retransfected with H77S.3/GLuc2A RNA. (A) Immunoblots of IGF2BP1, hnRNP L, ADAR1, DHX9, and NF90 72 h after siRNA transfection. β-Actin was included as a loading control. The percent depletion of each protein is shown. (B) Relative GLuc activity in supernatant fluids from Huh-7.5 cells transfected with HCV RNA and the indicated siRNAs. The results shown represent the means of three replicate experiments ± the standard deviations. Values at 6 h were arbitrarily set to 100. **, $P < 0.01$ (compared to si-Ctrl by two-way analysis of variance [ANOVA]). (C) WST-1 assay measurement of proliferation of cells transfected with indicated siRNAs at 72 h after HCV RNA transfection. Values for control siRNA were arbitrarily set to 100. **, $P < 0.01$ (compared to si-Ctrl by two-way ANOVA with Bonferroni's multiple-comparison test.)

in cell proliferation (Fig. 3C). We confirmed these results by infecting Huh-7.5 cells with HJ3-5 virus, an HCV genotype 1a/2a chimera that efficiently replicates and produces infectious particles in cell culture. Knockdown of hnRNP L dramatically diminished HJ3-5 replication, as measured by expression of HCV core and NS5A proteins; knockdown of NF90 also modestly reduced the abundance of core and NS5A proteins (Fig. 3D). Consistently, hnRNP L and NF90 knockdown resulted in 3- and 1.5-fold reductions in infectious virus yield after 72 h compared to cells transfected with a nontargeting control siRNA (Fig. 3E). The above-described experiments used siRNA pools targeting hnRNP L and NF90. To assess the possibility that inhibition of replication resulted from off-target effects of these siRNAs, we compared the knockdown efficiency of individual siRNAs with their impact on viral replication. We observed substantial variation in the capacity of individual siRNAs to deplete hnRNP L or NF90 (Fig. 3F), but with both proteins the degree of depletion strongly correlated with the magnitude of the reduction in HCV replication, as measured by GLuc assay (Fig. 3G). Thus, the reduction of HCV replication was likely caused by specific depletion of hnRNP L and NF90 and not spurious off-target effects of the siRNA. Collectively, these data strongly suggest a role for hnRNP L and NF90 in efficient HCV genome amplification.

To examine whether hnRNP L and NF90 are required for HCV IRES-mediated translation, we transfected cells with an HCV minigenome RNA comprised of the HCV 5′UTR and 3′UTR flanking the GLuc sequence as reporter (Fig. 4A). This RNA was transfected into Huh-7.5 cells depleted of hnRNP L and NF90, and secreted GLuc activity was measured over the ensuring 24 h. Depletion of hnRNP L and NF90 resulted in little difference in GLuc activity (Fig. 4B) or GLuc mRNA abundance at 24 h (Fig. 4C). These data suggest that hnRNP L and NF90 are not essential for HCV IRES-mediated translation and that they do not significantly influence the stability of RNAs containing the HCV 5′UTR. Since hnRNP L binds to the 5′ end of HCV RNA in competition with miR-122 (Fig. 1F), while NF90 binds nearby, we also tested whether hnRNP L and NF90 depletion would affect the capacity of miR-122 to promote HCV replication. We transfected H77S.3/GLuc2A RNA into control, hnRNP L- or NF90-depleted cells, together with miR-122 or miR-124. Consistent with previous reports (9, 10), miR-122 supplementation resulted in an ~2-fold increase in GLuc activity compared to a control miRNA, miR-124 (Fig. 4D). The fold increase in GLuc activity caused by miR-122 supplementation (2.06) was unchanged in hnRNP L- and NF90-depleted cells (1.95 to 2.06, Fig. 4D), indicating that significant reductions in hnRNP L and NF90 abundance do not influence miR-122 enhancement of HCV replication.

hnRNP L and NF90 have been reported to be nuclear proteins (29–31). We confirmed this by laser-scanning confocal fluorescence microscopy (data not shown). However, since the HCV life cycle is restricted to the cytoplasm, we further analyzed the distribution of hnRNP L and NF90 in Huh-7.5 cells by cytoplasmic-nuclear fractionation. As shown in Fig. 5A, hnRNP L was largely localized to the nuclear fraction, and yet a small proportion of it was present in cytoplasm. Approximately half of the NF90 abundance localized to the cytoplasm, while NF110, an isoform of NF90, was predominantly detected in the nuclear fraction. NF90 and NF110 share antigenic specificity, and this likely explains the discrepant microscopy findings. HCV infection did not alter the intracellular distribution of hnRNP L or NF90 (Fig. 5A, right).

To determine whether hnRNP L and NF90 bind to HCV RNA in infected cells, as they do *in vitro* (Fig. 1), we immunoprecipitated hnRNP L and NF90 from HJ3-5 virus-infected Huh-7.5 cells and examined the precipitate for the presence of viral RNA. hnRNP L and NF90 were efficiently pulled down by specific antibodies compared to an isotype control IgG (Fig. 5B). RNA coprecipitating with hnRNP L and NF90 was purified and HCV RNA amplified and detected by RT-PCR. As shown in Fig. 5B, HCV RNA coprecipitated with both hnRNP L and NF90, indicating that hnRNP L and NF90 associate with HCV RNA within infected cells. In contrast, antibody to Dcp1a, an mRNA-decapping protein that does not colocalize with HCV RNA in cells (10), did not pull down HCV RNA. hnRNP L and NF90 were also found to coprecipitate with NS5A in HCV-infected cells by immunoblot assay (Fig. 5C). This association was RNA dependent since RNase treatment completely abolished the interaction (Fig. 5C). To determine whether the RNA mediating the interaction between NS5A and hnRNP L or NF90 is HCV specific, we repeated this

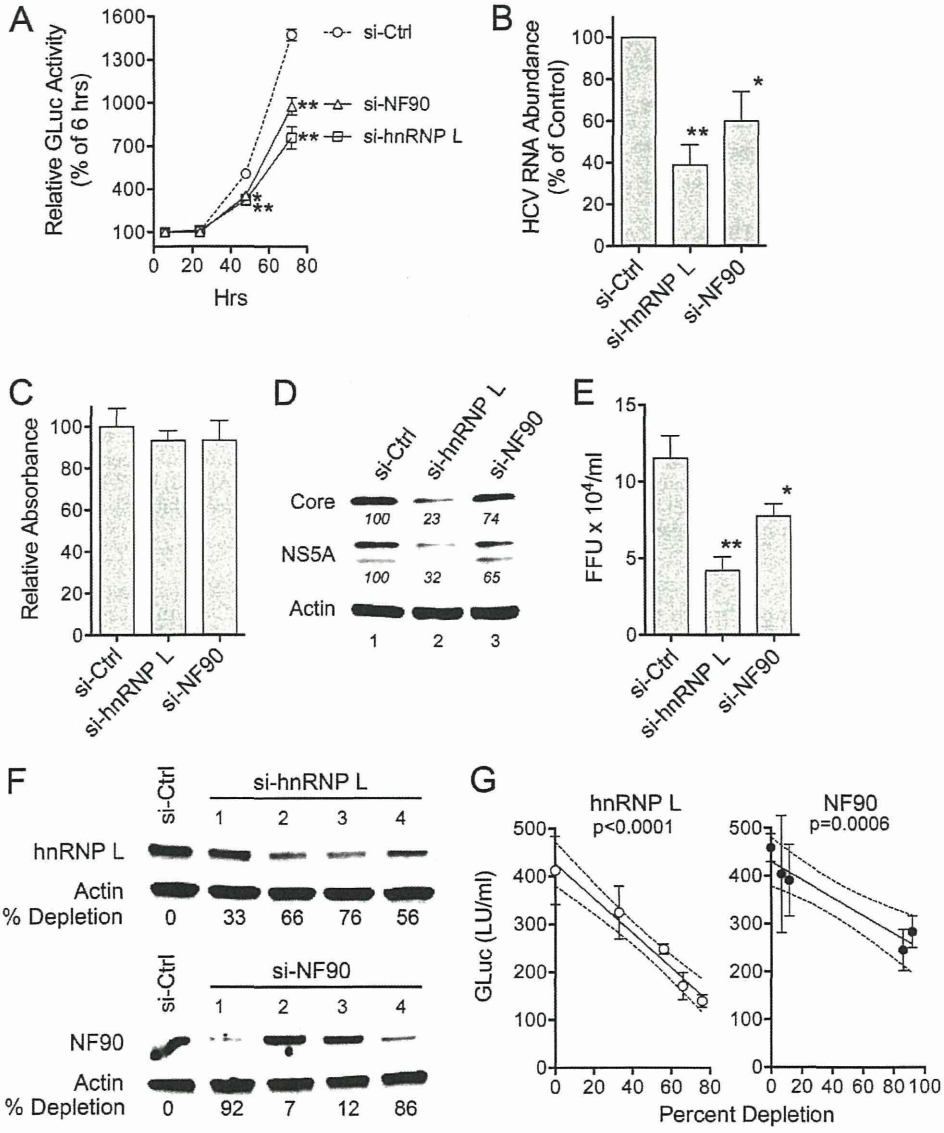

FIG 3 hnRNP L and NF90 are required for efficient HCV replication. (A) Huh-7.5 cells were maintained in growth media containing 2% serum, and transfected with siRNAs for hnRNP L, NF90, or scrambled si-Ctrl and then 48 h later retransfected with H77S.3/GLuc2A RNA. Supernatant fluids were removed at intervals and assayed for GLuc activity. Values at 6 h were arbitrarily set to 100. The results shown represent the means of three replicate experiments ± the standard errors of the mean. *, $P < 0.05$; **, $P < 0.01$ (compared to si-Ctrl by two-way ANOVA). (B) HCV RNA was quantified relative to β-actin mRNA by real-time RT-PCR 72 h after HCV RNA transfection. *, $P < 0.05$; **, $P < 0.01$ (compared to si-Ctrl by one-way ANOVA with Bonferroni's correction for multiple comparisons). (C) WST-1 assay for measurement of proliferation of cells at 72 h after HCV RNA transfection. Values for control siRNA were arbitrarily set to 100. Values do not differ significantly from si-CTRL (one-way ANOVA with Bonferroni's post test). (D) Immunoblots of HCV core and NS5A proteins at 72 h postinfection, with β-actin as a loading control. Huh-7.5 cells were maintained in growth medium containing 2% serum and transfected with siRNAs for hnRNP L, NF90, or scrambled si-Ctrl and then 48 h later infected with HJ3-5 virus. Italicized labels show quantification of core and NS5A proteins relative to β-actin, with values for si-Ctrl arbitrarily set to 100. (E) The infectious virus titers of supernatant fluids from panel D were determined by a fluorescent focus formation assay. The results shown represent the means of three replicate experiments ± the standard deviations. *, $P < 0.05$; **, $P < 0.01$ (compared to si-Ctrl by one-way ANOVA with Bonferroni's post test). (F) Individual siRNAs targeting hnRNP L or NF90 (four each) were transfected into cells, and hnRNP L and NF90 protein abundance was determined by immunoblotting 96 h later. β-Actin was included as a loading control. hnRNP L and NF90 levels were normalized to β-actin, and the percent depletion compared to si-Ctrl was calculated for each siRNA. (G) H77S.3/GLuc2A RNA was transfected into the hnRNP L- and NF90-depleted cells shown in panel F, and GLuc activity secreted from the cells between 48 and 72 h was assessed. The results shown represent mean GLuc ± the standard deviations in three replicate cultures, plotted against the percent depletion of target protein. Dashed lines represent the outer limits of the 95% confidence-interval band for a best-fit plot. The *P* values indicate the likelihood that the slope of this line diverges from "0". Inhibition of HCV replication was highly correlated with the degree of depletion of hnRNP L and NF90.

assay using U2OS cells that conditionally express only the NS5A protein (Fig. 5D). Little interaction was evident between NS5A and hnRNP L or NF90 under these conditions (Fig. 5E), suggesting that the coprecipitation of hnRNP L and NF90 with NS5A in infected cells may be largely mediated by HCV RNA. We found no evidence that either protein directly interacts with NS5A.

Previous studies indicate that HCV RNA replication complexes are localized to detergent-resistant intracellular mem-

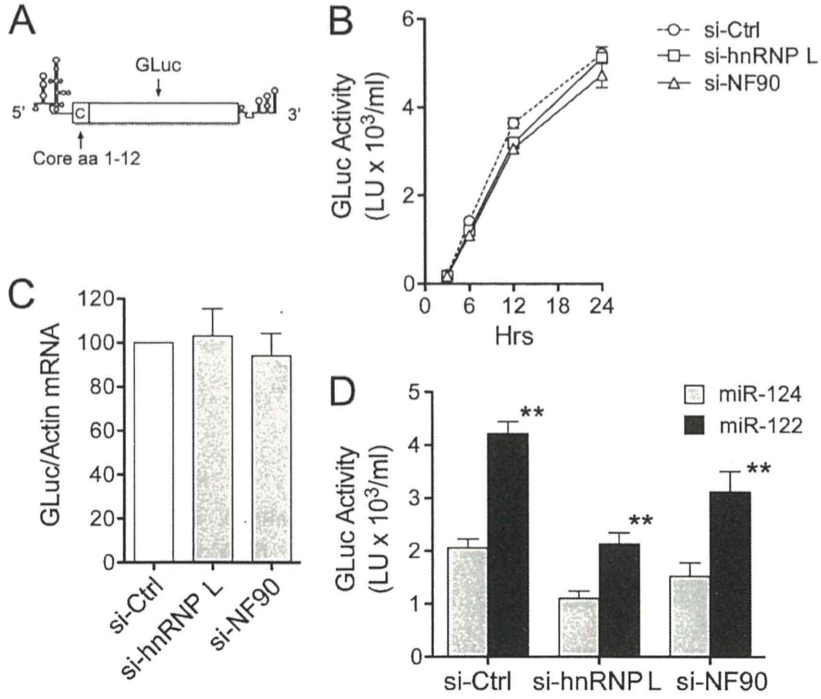

FIG 4 hnRNP L and NF90 depletion do not affect HCV IRES translation or miR-122 enhancement of HCV replication. (A) Diagram of the HCV minigenome RNA comprising the HCV 5′UTR followed by N-terminal core protein sequence fused to GLuc and the HCV 3′ UTR. (B) Huh-7.5 cells were transfected with siRNAs for hnRNP L, NF90 or scrambled si-Ctrl, and then 48 h later retransfected with HCV minigenome RNA. GLuc activity in supernatant fluids was measured at indicated times. The results shown represent the means of three replicate experiments ± the standard deviations. Values at 3 h were arbitrarily set to 100. (C) GLuc RNA levels were determined by real-time RT-PCR 24 h after HCV minigenome RNA transfection relative to β-actin mRNA. The differences in GLuc activity between hnRNP L- and NF90-depleted cells and cells transfected with si-Ctrl at 24 h (see panel B) were not significant when normalized to mRNA abundance ($P > 0.05$ as determined by two-sided t test). (D) Huh-7.5 cells were transfected with siRNAs for hnRNP L, NF90, or scrambled si-Ctrl and then 48 h later retransfected with H77s-GLuc RNA, together with 100 nM duplex miR-122 or miR-124. The GLuc activities were measured 72 h later. The results shown represent the means of three replicate experiments ± the standard deviations. **, $P < 0.01$ (compared to miR-124 by two-sided t test).

branes (DRMs) (32). Thus, to examine the possibility that hnRNP L and NF90 might be associated with replication complexes, we investigated their distribution within membrane fractions recovered from a flotation gradient. Cytoplasmic membranes from uninfected or HJ3-5 virus-infected Huh-7.5 cells were treated with Triton X-100, overlaid with a density gradient, and subjected to centrifugation (see Methods). Partitioning of DRMs and detergent soluble membranes (DSM) into separate fractions was confirmed by distinct distributions of caveolin-2 and calrecticulin among these fractions (Fig. 6A). HCV replication complexes were largely associated with the DRM, as shown by the distribution of NS5A. Although hnRNP L and NF90 were readily detected in DRM fractions from uninfected cells (3.0 to 6.85% and 2.2 to 3.2% of the total of hnRNP L and NF90, respectively, in the gradient were present in fractions 1 to 4), HCV infection increased the proportion of the proteins associating with the DRM (10.0 to 21.9% hnRNP L and 12.7 to 27.6% NF90 in replicate experiments) (Fig. 6A and B). In contrast, IGF2BP1, which binds nonspecifically to our RNA bait (Fig. 1D) and the depletion of which had relatively little effect on HCV replication (Fig. 2B), was barely detectable in DRM fractions, and its distribution was not altered by HCV infection (Fig. 6A). These data indicate that HCV infection results in an increased association of hnRNP L and NF90 with DRMs, providing additional evidence that these proteins are likely to be associated with the replication complex.

To further confirm this association, we treated the DRM fractions with proteinase K. Proteins present within membranous vesicles within the DRM fraction should be resistant to proteases in the absence of strong detergents. hnRNP L and NF90 in DRM fractions from uninfected cells were completely digested by proteinase K (Fig. 6C), indicating that they are not protected by membranes. In contrast, a significant fraction of hnRNP L and NF90 in DRM fractions from HCV-infected cells was resistant to protease treatment (Fig. 6C). Pretreatment of these fractions with 1% NP-40, which should disrupt all membrane structures, rendered these proteins sensitive to proteinase K. Taken together with the increased distribution of hnRNP L and NF90 into the DRM fractions (Fig. 6A and B), these data suggest that hnRNP L and NF90 are recruited into replication complexes to facilitate replication.

DISCUSSION

The 5′-terminal sequence of the HCV genome contains two miR-122 binding sites and is known to have an important regulatory role in viral RNA replication (3, 4, 19). The predicted secondary structure of the 47-nucleotide terminal sequence contains a conserved stem-loop (SLI), followed by an unstructured region within which the miR-122 seed sequence-binding sites are located (Fig. 1A, left). We hypothesized that these conserved regions may interact with host proteins that regulate viral RNA translation and/or replication. To assess this hypothesis, we used a biotin-RNA pulldown strategy to identify proteins that bind to this 5′-terminal sequence. In addition to Ago2 and PCBP2, which have

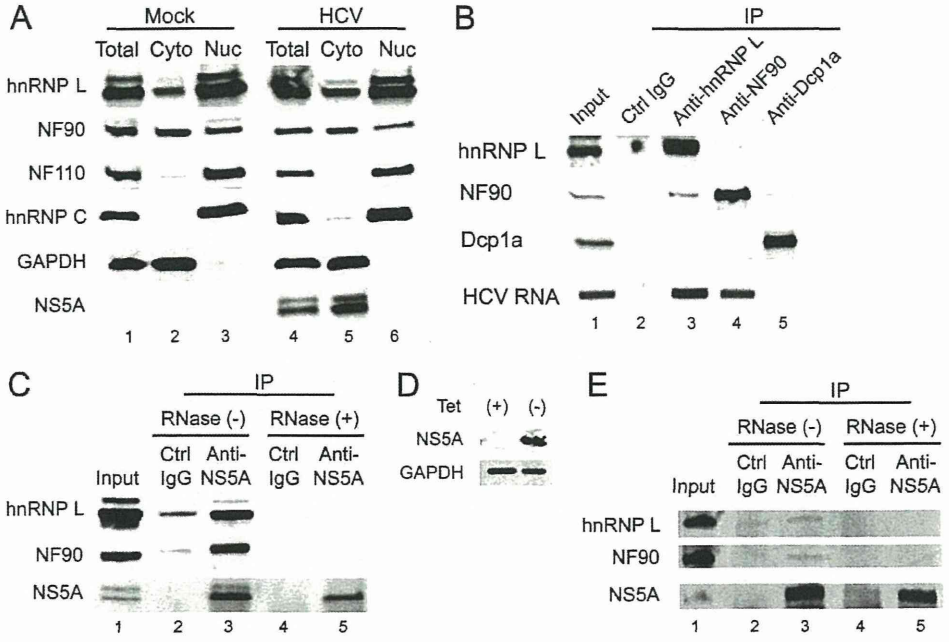

FIG 5 Cellular localization and association of hnRNP L and NF90 with HCV RNA and NS5A. (A) Distribution of hnRNP L and NF90 in cytoplasmic and nuclear fractions. Total lysate and cytoplasmic and nuclear fractions of Huh-7.5 cells with or without HCV infection were prepared, and the distribution of the indicated proteins was assessed using immunoblotting. hnRNP L was largely localized to the nuclear fraction, with a small amount in the cytoplasm. NF90 protein was equally distributed between cytoplasmic and nuclear fractions, while NF110, an isoform of NF90, predominantly localized to the nucleus. GAPDH (glyceraldehyde-3-phosphate dehydrogenase) was used as cytoplasmic marker and hnRNP C as a nuclear marker. HCV NS5A protein was detected only in the cytoplasmic fraction from infected cells. (B) hnRNP L and NF90 associate with HCV RNA in infected cells. hnRNP L or NF90 proteins were immunoprecipitated by specific antibodies from a cytoplasmic lysate of Huh-7.5 cells infected with HJ3-5 virus. Precipitation of hnRNP L and NF90 proteins was confirmed by immunoblotting. RNAs were extracted from the precipitates, and HCV RNA was detected by RT-PCR. Isotype control IgG was used as negative control. 5% input lysate was loaded as a reference. (C) RNA-dependent association of NS5A with hnRNP L and NF90. NS5A protein was immunoprecipitated by specific antibody or control IgG from HJ3-5 virus-infected Huh-7.5 cytoplasmic lysate with or without RNase treatment. NS5A, hnRNP L, and NF90 proteins in the precipitates were detected by immunoblotting. 5% input lysate was loaded as reference. hnRNP L and NF90 coimmunoprecipitate with NS5A only in non-RNase-treated samples. (D) U2OS cells with tet-regulated expression of NS5A protein were treated with or without 2 μg of tetracycline/ml for 48 h, and the expression of NS5A was detected by immunoblotting with GAPDH as a loading control. (F) NS5A immunoprecipitation was carried out as in panel C for U2OS cells expressing NS5A protein. Little coprecipitation of hnRNP L and NF90 with NS5A was observed.

been shown previously to bind this region of the genome (9, 14, 20), we documented the binding of several novel proteins, including hnRNP L, DHX9, ADAR1, and NF90 (Fig. 1B and C). hnRNP L binds ssRNA, whereas DHX9, ADAR1, and NF90 bind the double-strand complement of this RNA segment. Among these proteins, siRNA-mediated knockdowns of either hnRNP L or NF90 reduced HCV RNA and protein levels within infected cells (Fig. 3), suggesting that both are required for efficient HCV replication. hnRNP L and NF90 function in the HCV life cycle independently of miR-122, because depletion of either did not affect the capacity of miR-122 to stimulate HCV replication (Fig. 4D). hnRNP L and NF90 depletion had no impact on GLuc activity expressed by an HCV minigenome (Fig. 4B), suggesting they are not required for HCV IRES-mediated translation.

Previous studies have demonstrated that HCV RNA replication complexes consist of viral and host proteins assembled on DRMs (32). The localization of hnRNP L and NF90 to the DRM fractions of HCV-infected cells (Fig. 6A and B) thus suggests that they may be associated with the RNA replication complex. The fact that both proteins are protected by membranes from protease digestion in these DRM fractions provides further support for this (Fig. 6C). Immunoprecipitation of hnRNP L and NF90 in HCV-infected cells confirmed their association with HCV RNA (Fig. 5B). It is particularly interesting that hnRNP L and NF90 coimmunoprecipitated with NS5A (Fig. 5C), an essential component of the replication complex. The interaction was dependent on RNA, suggesting that while hnRNP L and NF90 do not physically interact with NS5A, they may form an RNA-protein complex together, possibly in association with HCV RNA in the replication complex.

hnRNPs are proteins that interact with heterogeneous nuclear RNAs (hnRNAs) (33). Several functions have been suggested for hnRNPs, including pre-mRNA processing, mRNA translocation from the nucleus to the cytoplasm, and translation (33). This group of RNA-binding proteins has been shown to participate in both viral IRES mediated-translation and viral replication. For example, PTB (hnRNP I) has been shown to enhance IRES-dependent translation of encephalomyocarditis virus and foot-and-mouth disease virus, both picornaviruses, as well as HCV (16, 34, 35). PCBP2 (hnRNP E2) is required for efficient translation and replication of both poliovirus and HCV RNA (14, 36). hnRNP L has been reported to be localized mainly in the nucleus (29). However, we detected hnRNP L in the cytoplasm both in the presence and in the absence of HCV infection (Fig. 5), suggesting that it may shuttle between the nucleus and cytoplasm. hnRNP L was previously reported to be required for HCV IRES-dependent translation because an RNA aptamer specific for hnRNP L blocked reporter protein translation directed by the HCV IRES

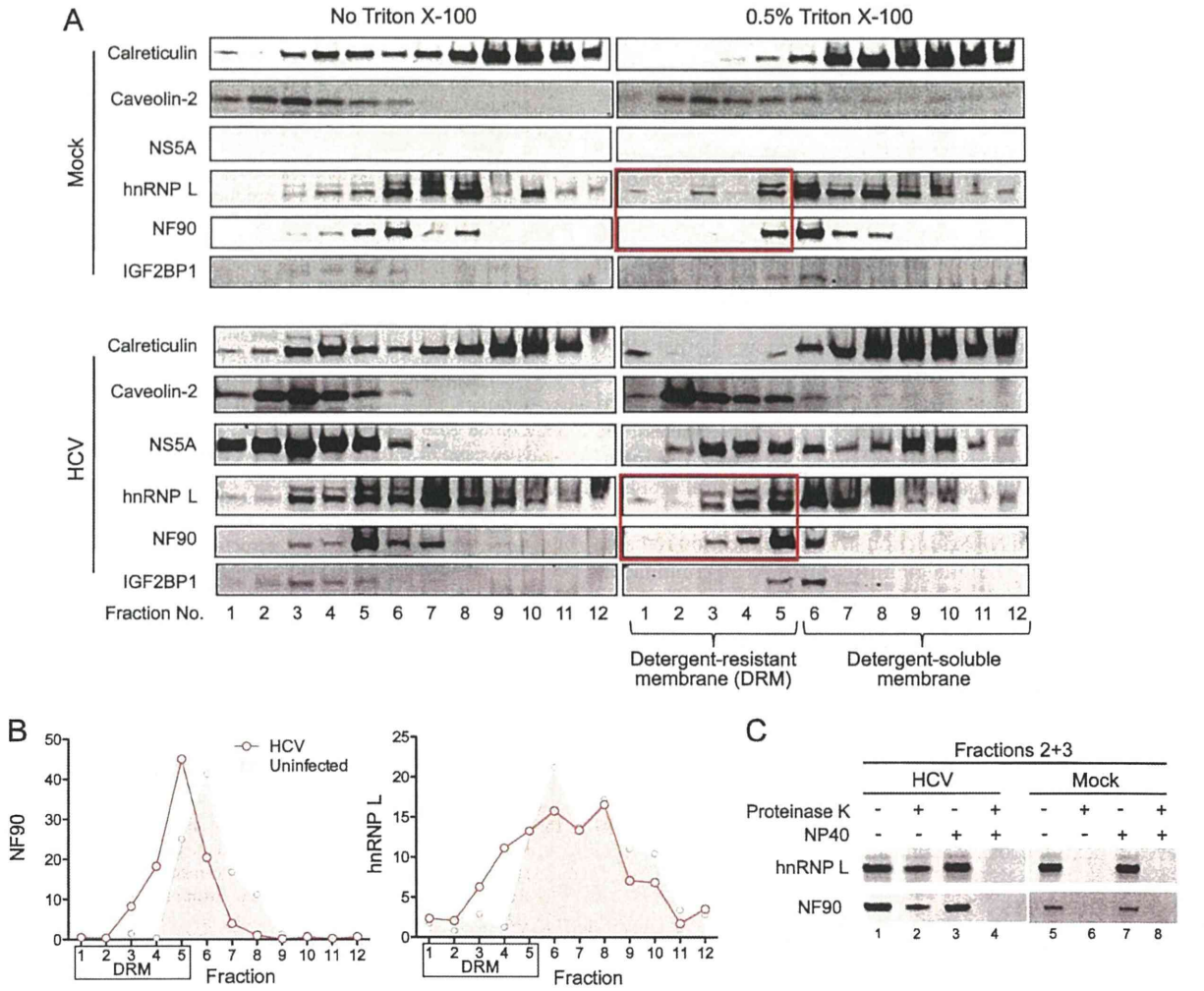

FIG 6 Membrane flotation assay. (A) Analysis of the distribution of hnRNP L and NF90 in fractions recovered from a membrane flotation assay. Cytoplasmic membranes extracted from FT3-7 cells with or without HCV infection were treated or not treated with Triton X-100, overlaid with a density gradient, and subjected to centrifugation. Fractions were subsequently recovered from the top of the gradient, and proteins in each were precipitated, resolved by SDS-PAGE, and analyzed by immunoblotting. Calrecticulin and caveolin-2 were detected as markers for detergent-soluble membrane (DSM) and detergent-resistant membrane (DRM), respectively. A substantial proportion of NS5A was located in DRM fractions, consistent with its presence in the HCV replication complex. hnRNP L and NF90 were readily detected in DRM, while little IGF2BP1 protein was found present in DRM. The image shown is representative of replicate experiments. (B) Quantification of the distribution of hnRNP L and NF90 proteins in fractions from the flotation gradients shown in panel A. Protein bands in immunoblots of each fraction were quantified with an Odyssey infrared imaging system. (C) hnRNP L and NF90 distributed to the DRM are protected from protease digestion in gradients loaded with material from HCV-infected cells. Fractions 2 and 3 (no Triton X-100) from panel A were treated with proteinase K with or without prior treatment with 1% NP-40. hnRNP L and NF90 proteins were detected by immunoblotting. hnRNP L and NF90 were uniformly sensitive to protease K in uninfected cells, whereas hnRNP L and NF90 associating with the DRM were resistant to proteinase K in HCV-infected cells. All proteins in fractions 8 and 9 from either uninfected or infected cells were sensitive to protease treatment (data not shown).

(37). However, in our study hnRNP L had little effect on the translation of a minigenome reporter containing both HCV UTRs, indicating that it is not essential for HCV IRES-dependent translation initiation (Fig. 4). It is possible the aptamer used in the previous report caused a nonspecific inhibition of IRES activity.

It is intriguing that the hnRNP L protein binding site appears to overlap with miR-122 binding sites in HCV 5′UTR, since the p6 mutation in the S1 and S2 sites reduced hnRNP L binding to the RNA bait in the pulldown experiments (Fig. 1E). However, the binding of hnRNP L to the HCV 5′ terminus is independent of miR-122, since the anti-miR-122 antagomir did not block binding of hnRNP L (Fig. 1F). In contrast, preincubation of the RNA bait with miR-122 diminished hnRNP L binding, indicating that hnRNP L and miR-122 bind competitively to overlapping sites. It is puzzling why two proviral factors, miR-122 and hnRNP L, would compete with each other. One plausible explanation is that hnRNP L and miR-122 are involved in different stages of the HCV life cycle and that a change of binding factors at the 5′ RNA terminus is accompanied by a transition between these different stages. Further work will be required to investigate this hypothesis.

NF90 belongs to a family of proteins that contain a double-strand RNA binding motif and exert a variety of functions involving RNA recognition, RNA processing, and RNA stability (38). NF90 has previously been reported to form a complex with DHX9

(39). Although DHX9 and NF90 both bound to the dsRNA bait (Fig. 1), depletion of NF90 had a much greater impact on HCV replication (Fig. 2B). NF90 has been shown to positively regulate replication of several positive-strand RNA virus, including dengue virus and bovine viral diarrhea virus, a pestivirus closely related to HCV (40, 41). This suggests its host factor function may be conserved among the *Flaviviridae*. It binds to the 5′UTRs and/or 3′UTRs of these viruses and promotes their replication. It has also been reported to associate with both the 5′UTRs and 3′UTRs of HCV in a cross-linking assay and to promote interactions between the 5′ and 3′ ends of the genome (42). Although we found that NF90 bound to the dsRNA bait (Fig. 1) and was required for efficient HCV replication (Fig. 3), we do not know whether NF90 mediates HCV replication through its direct association with dsRNA (as we have demonstrated) or by binding to structured elements within the HCV 5′UTRs and 3′UTRs. Nevertheless, the increased distribution of NF90 into DRM following HCV infection (Fig. 6) suggests the association of NF90 with viral replicase complexes.

How hnRNP L and NF90 function in HCV replication remains to be determined. The binding of hnRNP L or NF90 could facilitate replication complex assembly by recruiting other viral and host factors onto HCV RNA or possibly induce conformational changes in the RNA that promote viral RNA synthesis. Further studies are needed to dissect the individual steps in the viral life cycle impacted by hnRNP L and NF90 and to identify other host and viral proteins involved. Further elucidation of the molecular basis of the function of hnRNP L and NF90 on HCV replication could yield important insight into unrecognized actions of RNA-binding proteins in the viral life cycle and possibly provide clues for development of broadly acting antiviral therapies.

ACKNOWLEDGMENTS

This study was supported in part by National Institutes of Health grants R01-AI095690 and R01-CA164029. Additional support was provided by the Lineberger Comprehensive Cancer Center (P30-CA16086) and the University Cancer Research Fund of the University of North Carolina.

We thank Takaji Wakita for the gift of rabbit antibody to NS5A, Darius Moradpour for the gift of cells with Tet-regulated expression of NS5A, and the staff of the UNC Proteomics Core Facility for their assistance with mass spectrometry.

REFERENCES

1. Chang J, Nicolas E, Marks D, Sander C, Lerro A, Buendia MA, Xu C, Mason WS, Moloshok T, Bort R, Zaret KS, Taylor JM. 2004. miR-122, a mammalian liver-specific microRNA, is processed from hcr mRNA and may downregulate the high-affinity cationic amino acid transporter CAT-1. RNA Biol. 1:106–113. http://dx.doi.org/10.4161/rna.1.2.1066.
2. Jopling CL, Yi M, Lancaster AM, Lemon SM, Sarnow P. 2005. Modulation of hepatitis C virus RNA abundance by a liver-specific microRNA. Science 309:1577–1581. http://dx.doi.org/10.1126/science.1113329.
3. Jopling CL, Schütz S, Sarnow P. 2008. Position-dependent function for a tandem microRNA miR-122-binding site located in the hepatitis C virus RNA genome. Cell Host Microbe 4:77–85. http://dx.doi.org/10.1016/j.chom.2008.05.013.
4. Jangra RK, Yi M, Lemon SM. 2010. miR-122 regulation of hepatitis C virus translation and infectious virus production. J. Virol. 84:6615–6625. http://dx.doi.org/10.1128/JVI.00417-10.
5. Janssen HL, Reesink HW, Lawitz EJ, Zeuzem S, Rodriguez-Torres M, Patel K, van der Meer AJ, Patick AK, Chen A, Zhou Y, Persson R, King BD, Kauppinen S, Levin AA, Hodges MR. 2013. Treatment of HCV infection by targeting microRNA. N. Engl. J. Med. 368:1685–1694. http://dx.doi.org/10.1056/NEJMoa1209026.
6. Lanford RE, Hildebrandt-Eriksen ES, Petri A, Persson R, Lindow M, Munk ME, Kauppinen S, Orum H. 2010. Therapeutic silencing of microRNA-122 in primates with chronic hepatitis C virus infection. Science 327:198–201. http://dx.doi.org/10.1126/science.1178178.
7. Henke JI, Goergen D, Zheng J, Song Y, Schuttler CG, Fehr C, Junemann C, Niepmann M. 2008. microRNA-122 stimulates translation of hepatitis C virus RNA. EMBO J. 27:3300–3310. http://dx.doi.org/10.1038/emboj.2008.244.
8. Jangra RK, Yi M, Lemon SM. 2010. Regulation of hepatitis C virus translation and infectious virus production by the microRNA miR-122. J. Virol. 84:6615–6625. http://dx.doi.org/10.1128/JVI.00417-10.
9. Shimakami T, Yamane D, Jangra RK, Kempf BJ, Spaniel C, Barton DJ, Lemon SM. 2012. Stabilization of hepatitis C RNA by an Ago2-miR-122 complex. Proc. Natl. Acad. Sci. U. S. A. 109:941–946. http://dx.doi.org/10.1073/pnas.1112263109.
10. Li Y, Masaki T, Yamane D, McGivern DR, Lemon SM. 2013. Competing and noncompeting activities of miR-122 and the 5′ exonuclease Xrn1 in regulation of hepatitis C virus replication. Proc. Natl. Acad. Sci. U. S. A. 110:1881–1886. http://dx.doi.org/10.1073/pnas.1213515110.
11. Conrad KD, Giering F, Erfurth C, Neumann A, Fehr C, Meister G, Niepmann M. 2013. microRNA-122-dependent binding of Ago2 protein to hepatitis C virus RNA Is associated with enhanced RNA stability and translation stimulation. PLoS One 8:e56272. http://dx.doi.org/10.1371/journal.pone.0056272.
12. Fraser CS, Doudna JA. 2007. Structural and mechanistic insights into hepatitis C viral translation initiation. Nat. Rev. Microbiol. 5:29–38. http://dx.doi.org/10.1038/nrmicro1558.
13. Honda M, Beard MR, Ping LH, Lemon SM. 1999. A phylogenetically conserved stem-loop structure at the 5′ border of the internal ribosome entry site of hepatitis C virus is required for cap-independent viral translation. J. Virol. 73:1165–1174.
14. Wang L, Jeng KS, Lai MM. 2011. Poly(C)-binding protein 2 interacts with sequences required for viral replication in the hepatitis C virus (HCV) 5′ untranslated region and directs HCV RNA replication through circularizing the viral genome. J. Virol. 85:7954–7964. http://dx.doi.org/10.1128/JVI.00339-11.
15. Ali N, Siddiqui A. 1997. The La antigen binds 5′ noncoding region of the hepatitis C virus RNA in the context of the initiator AUG codon and stimulates internal ribosome entry site-mediated translation. Proc. Natl. Acad. Sci. U. S. A. 94:2249–2254. http://dx.doi.org/10.1073/pnas.94.6.2249.
16. Ali N, Siddiqui A. 1995. Interaction of polypyrimidine tract-binding protein with the 5′ noncoding region of the hepatitis C virus RNA genome and its functional requirement in internal initiation of translation. J. Virol. 69:6367–6375.
17. Buratti E, Tisminetzky S, Zotti M, Baralle FE. 1998. Functional analysis of the interaction between HCV 5′UTR and putative subunits of eukaryotic translation initiation factor eIF3. Nucleic Acids Res. 26:3179–187. http://dx.doi.org/10.1093/nar/26.13.3179.
18. Sizova DV, Kolupaeva VG, Pestova TV, Shatsky IN, Hellen CU. 1998. Specific interaction of eukaryotic translation initiation factor 3 with the 5′ nontranslated regions of hepatitis C virus and classical swine fever virus RNAs. J. Virol. 72:4775–4782.
19. Friebe P, Lohmann V, Krieger N, Bartenschlager R. 2001. Sequences in the 5′ nontranslated region of hepatitis C virus required for RNA replication. J. Virol. 75:12047–12057. http://dx.doi.org/10.1128/JVI.75.24.12047-12057.2001.
20. Fukushi S, Okada M, Kageyama T, Hoshino FB, Nagai K, Katayama K. 2001. Interaction of poly(rC)-binding protein 2 with the 5′-terminal stem-loop of the hepatitis C-virus genome. Virus Res. 73:67–79. http://dx.doi.org/10.1016/S0168-1702(00)00228-8.
21. Shimakami T, Yamane D, Welsch C, Hensley L, Jangra RK, Lemon SM. 2012. Base pairing between hepatitis C Virus RNA and microRNA 122 3′ of its seed sequence is essential for genome stabilization and production of infectious virus. J. Virol. 86:7372–7383. http://dx.doi.org/10.1128/JVI.00513-12.
22. Moradpour D, Kary P, Rice CM, Blum HE. 1998. Continuous human cell lines inducibly expressing hepatitis C virus structural and nonstructural proteins. Hepatology 28:192–201. http://dx.doi.org/10.1002/hep.510280125.
23. Shimakami T, Welsch C, Yamane D, McGivern D, Yi M, Zeuzem S, Lemon SM. 2011. Protease inhibitor-resistant hepatitis C virus mutants with reduced fitness from impaired production of infectious virus. Gas-

troenterology 140:667–675. http://dx.doi.org/10.1053/j.gastro.2010.10.056.
24. Yi M, Villanueva RA, Thomas DL, Wakita T, Lemon SM. 2006. Production of infectious genotype 1a hepatitis C virus (Hutchinson strain) in cultured human hepatoma cells. Proc. Natl. Acad. Sci. U. S. A. 103:2310–2315. http://dx.doi.org/10.1073/pnas.0510727103.
25. Okamoto K, Mori Y, Komoda Y, Okamoto T, Okochi M, Takeda M, Suzuki T, Moriishi K, Matsuura Y. 2008. Intramembrane processing by signal peptide peptidase regulates the membrane localization of hepatitis C virus core protein and viral propagation. J. Virol. 82:8349–8361. http://dx.doi.org/10.1128/JVI.00306-08.
26. Weinlich S, Hüttelmaier S, Schierhorn A, Behrens SE, Ostareck-Lederer A, Ostareck DH. 2009. IGF2BP1 enhances HCV IRES-mediated translation initiation via the 3′UTR. RNA 15:1528–1542. http://dx.doi.org/10.1261/rna.1578409.
27. Bradrick SS, Nagyal S, Novatt H. 2013. A miRNA-responsive cell-free translation system facilitates isolation of hepatitis C virus miRNP complexes. RNA 19:1159–1169. http://dx.doi.org/10.1261/rna.038810.113.
28. Kao PN, Chen L, Brock G, Ng J, Kenny J, Smith AJ, Corthésy B. 1994. Cloning and expression of cyclosporin A- and FK506-sensitive nuclear factor of activated T cells: NF45 and NF90. J. Biol. Chem. 269:20691–20699.
29. Piñol-Roma S, Swanson MS, Gall JG, Dreyfuss G. 1989. A novel heterogeneous nuclear RNP protein with a unique distribution on nascent transcripts. J. Cell Biol. 109:2575–2587. http://dx.doi.org/10.1083/jcb.109.6.2575.
30. Sakamoto S, Aoki K, Higuchi T, Todaka H, Morisawa K, Tamaki N, Hatano E, Fukushima A, Taniguchi T, Agata Y. 2009. The NF90-NF45 complex functions as a negative regulator in the microRNA processing pathway. Mol. Cell. Biol. 29:3754–3769. http://dx.doi.org/10.1128/MCB.01836-08.
31. Barber GN. 2009. The NFAR's (nuclear factors associated with dsRNA): evolutionarily conserved members of the dsRNA binding protein family. RNA Biol. 6:35–39. http://dx.doi.org/10.4161/rna.6.1.7565.
32. Shi ST, Lee KJ, Aizaki H, Hwang SB, Lai MM. 2003. Hepatitis C virus RNA replication occurs on a detergent-resistant membrane that cofractionates with caveolin-2. J. Virol. 77:4160–4168. http://dx.doi.org/10.1128/JVI.77.7.4160-4168.2003.
33. Han SP, Tang YH, Smith R. 2010. Functional diversity of the hnRNPs: past, present, and perspectives. Biochem. J. 430:379–392. http://dx.doi.org/10.1042/BJ20100396.
34. Kaminski A, Hunt SL, Patton JG, Jackson RJ. 1995. Direct evidence that polypyrimidine tract binding protein (PTB) is essential for internal initiation of translation of encephalomyocarditis virus RNA. RNA 1:924–938.
35. Niepmann M. 1996. Porcine polypyrimidine tract-binding protein stimulates translation initiation at the internal ribosome entry site of foot-and-mouth-disease virus. FEBS Lett. 388:39–42. http://dx.doi.org/10.1016/0014-5793(96)00509-1.
36. Blyn LB, Towner JS, Semler BL, Ehrenfeld E. 1997. Requirement of poly(rC) binding protein 2 for translation of poliovirus RNA. J. Virol. 71:6243–6246.
37. Hwang B, Lim JH, Hahm B, Jang SK, Lee SW. 2009. hnRNP L is required for the translation mediated by HCV IRES. Biochem. Biophys. Res. Commun. 378:584–588. http://dx.doi.org/10.1016/j.bbrc.2008.11.091.
38. Tian B, Bevilacqua PC, Diegelman-Parente A, Mathews MB. 2004. The double-stranded-RNA-binding motif: interference and much more. Nat. Rev. Mol. Cell. Biol. 5:1013–1023. http://dx.doi.org/10.1038/nrm1528.
39. Liao HJ, Kobayashi R, Mathews MB. 1998. Activities of adenovirus virus-associated RNAs: purification and characterization of RNA binding proteins. Proc. Natl. Acad. Sci. U. S. A. 95:8514–8519. http://dx.doi.org/10.1073/pnas.95.15.8514.
40. Gomila RC, Martin GW, Gehrke L. 2011. NF90 binds the dengue virus RNA 3′ terminus and is a positive regulator of dengue virus replication. PLoS One 6:e16687. http://dx.doi.org/10.1371/journal.pone.0016687.
41. Isken O, Grassmann CW, Sarisky RT, Kann M, Zhang S, Grosse F, Kao PN, Behrens SE. 2003. Members of the NF90/NFAR protein group are involved in the life cycle of a positive-strand RNA virus. EMBO J. 22:5655–5665. http://dx.doi.org/10.1093/emboj/cdg562.
42. Isken O, Baroth M, Grassmann CW, Weinlich S, Ostareck DH, Ostareck-Lederer A, Behrens SE. 2007. Nuclear factors are involved in hepatitis C virus RNA replication. RNA 13:1675–1692. http://dx.doi.org/10.1261/rna.594207.